Nanoscale Advances

ROYAL SOCIETY OF CHEMISTRY

PAPER

View Article Online
View Journal

Cite this: DOI: 10.1039/d6na00160b

Nano-$NiFe_2O_4$ as a versatile and recyclable catalyst: an efficient protocol for the synthesis of aryl-1,2,4-triazolidine-3-thiones under ball milling conditions

Pankaj V. Ledade, [ac] Trimurti L. Lambat, *[b] Jitendra K. Gunjate,[c] Pooja M. Kadu,[d] Utpal J. Dongre,[d] Amitkumar V. Bhute,[e] Twinkle S. Wankhede, [f] Sami H. Mahmood *[g] and Subhash Banerjee *[h]

Received 27th February 2026
Accepted 8th May 2026

DOI: 10.1039/d6na00160b

rsc.li/nanoscale-advances

In this research, the catalytic efficiency of nano-$NiFe_2O_4$ is examined in the production of aryl-1,2,4-triazolidine-3-thiones under ball-milling conditions. The reactions of thiosemicarbazides with a range of substrates, such as aryl and heteroaryl aldehydes, have been effectively shown to give the corresponding aryl-1,2,4-triazolidine-3-thiones under solvent-free conditions in a ball-milling method. This process is characterised by high EcoScale values and a relatively low E-factor. The methodology outlined in the present study follows the concepts of green chemistry, which include optimized ball milling conditions, shortened reaction times, increased product yields, recyclability of the catalyst, and high atom economy.

1 Introduction

Heterocyclic compounds are some of the most intriguing and important classes of organic molecules because of their abundance in a large range of natural products, pharmaceuticals, agrochemicals and functional materials.[1–3] Heterocycles containing nitrogen and sulphur have attracted a lot of attention due to their extensive range of biological functions and chemical reactivity.[4,5] Triazole and triazolidine analogues play a major role in medicinal chemistry because their structural alterations can have a considerable impact on their biological response.[6a–d–8] Green, safe and friendly synthetic procedures have been developed to suit the ever-growing requirement of structurally varied, physiologically active heterocyclic compounds.[9,10]

The aryl-1,2,4-triazolidine-3-thione nucleus, a reduced form of 1,2,4-triazole containing a thiocarbonyl (C=S) group, is very important in hydrogen bonding and biological interactions and the coordination of metals.[11a,b,12] Pharmacological activities of compounds with this moiety are excellent, and they consist of antifungal, antiviral, anticancer, antituberculous, and antimicrobial activities.[13–17] Sulphur and nitrogen make them more lipophilic, thereby enhancing their biological target binding capacity (Fig. 1). They are thus good alternatives when designing new drugs.[18a,b]

Biological activity is enhanced by the change in electronic and steric properties of the triazolidine ring at the position of the 5-aryl group.[19] Electron-contributing or withdrawing substituents of the aryl ring influence membrane permeability, receptor affinity and stability of metabolites.[20,21] Consequently, substituted-5-aryl-1, 2,4-triazolidine-3-thiones have emerged as interesting models in the development of new medicines.[22] Many investigations have demonstrated the high antimicrobial and antifungal effects of substituted triazolidine-3-thione analogs.[23,24] Some of the derivatives have a profound inhibitory effect on the growth of many species of *Aspergillus*, *Candida albicans*, *Staphylococcus aureus* and *Escherichia coli*.[25] The thiocarbonyl group is believed to interfere with the enzyme systems of the microbes through chelation or covalent interaction.[26]

These compounds have also been found to exhibit potent anticancer effects on a broad range of human cancer cell lines, including liver, colon, breast and lung cancer cell lines.[27] Their action mechanism is frequently to induce cell death, arrest the cell cycle and inhibit enzymes that promote tumour growth.[28] The heterocyclic structure acts as an antioxidant to remove free radicals and alleviate oxidative stress, which are two conditions

[a]Department of Chemistry, Yashwantrao Chawhan Arts, Commerce & Science College, Lakhandur, Bhandara 441803, Maharashtra, India
[b]Department of Chemistry, Manoharbhai Patel College of Arts, Commerce & Science, Deori, Gondia, 441901, Maharashtra, India. E-mail: lambatges@gmail.com
[c]Department of Chemistry, SSES Amravati's Science College, Congress Nagar, Nagpur 440012, Maharashtra, India
[d]Department of Biochemistry, Dr Ambedkar College, Deeksha Bhoomi, Nagpur, 440010, Maharashtra, India. E-mail: lambatges@gmail.com
[e]Post Graduate Teaching Department of Chemistry, Rashtrasant Tukadoji Maharaj Nagpur University, Nagpur 440033, Maharashtra, India
[f]Department of Chemistry, Dr Ambedkar College, Deeksha Bhoomi, Nagpur, 440010, Maharashtra, India
[g]Department of Physics, The University of Jordan, Amman 11942, Jordan. E-mail: s.mahmood@ju.edu.jo
[h]Department of Chemistry, Guru Ghasidas Vishwavidyalaya (A Central University), Koni, Bilaspur, 495009, Chhattisgarh, India. E-mail: ocsb2006@gmail.com

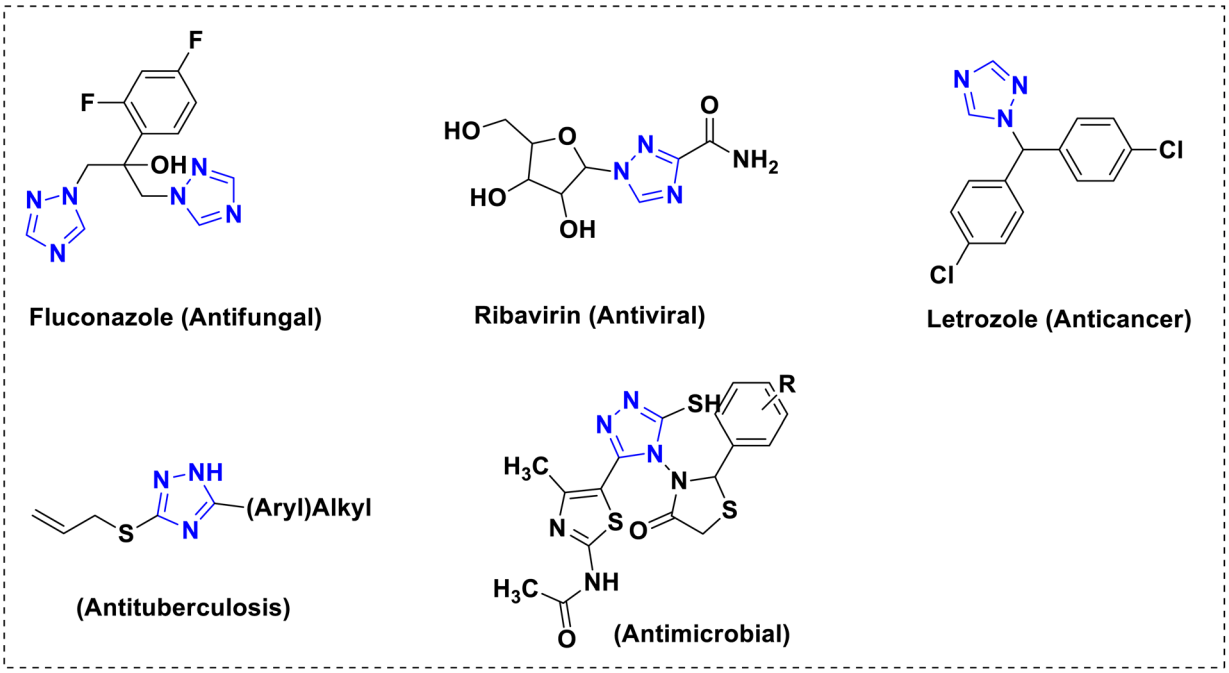

Fig. 1 A few compounds with 1,2,4-triazole groups that have pharmacological activity.

associated with chronic diseases such as cancer and neurological disorders.[29]

Moreover, 1,2,4-triazolidine-3-thione analogs are used as anti-inflammatory and analgesic agents in blocking the COX (cyclooxygenase) and lipoxygenase (LOX) pathways.[30] Some derivatives have been proven to be effective against TB and viruses, which points to the importance of this scaffold in medicine.[31–33] The variety of exemplified biological activities highlights the necessity to develop effective synthetic approaches for the production of a broad selection of substituted derivatives.

The significance of the synthesis of substituted triazolidine-3-thiones has been associated with the challenges of long reaction time, harsh conditions, excessive use of solvents, low yield, and the inability to reuse catalysts, which are associated with conventional methods used in the synthesis of substituted triazolidine-3-thiones.[34] Conventional heating systems demand high temperatures and long reflux periods, which consume more energy and thus lead to adverse environmental effects.[35]

The identified limitations are contrasted with the concepts of green chemistry, which strongly focus on utilizing non-toxic reagents, increased energy efficiency, minimized waste, and recyclable catalysts, which is apparent in the area of sustainable chemistry.[36,37] As a result, new synthetic approaches, which will be both environmentally friendly and economically viable, must be developed without affecting the efficiency of operations or the range of product diversification.

Mechanochemistry, of which the key modality is that of ball milling, has become a powerful and sustainable approach to the synthesis of organic compounds.[38,39] In ball milling, chemical transformations occur through the mechanical energy generated as the collisions between the milling media and the reactants take place.[40] This leads to solvents being either obviated or restricted to small amounts. Such a solvent-reducing strategy is in line with the values of green chemistry and has received significant academic interest in the past few years.[41,42]

The benefits of ball milling compared to traditional solution-phase synthesis are an increase in the reaction rate, improved yields, increased selectivity, and ease of operation. Besides, mechanochemical reactions often occur at room temperature, reducing energy use, thus avoiding the need for harmful solvents.[43] The mentioned features make ball milling an attractive method in the production of biologically relevant heterocyclic substances.[44]

The combination of nanocatalysis and mechanochemistry makes organic changes more sustainable and efficient to a significant extent.[45] Nanocatalysts have more active sites, a greater surface-to-volume ratio and more catalytic activity than their bulk counterparts.[46] Magnetic ferrite nanoparticles, including $NiFe_2O_4$, are especially an appealing type of nanomaterial; recently, they have been receiving extensive attention because of their high thermal stability, easy magnetic separation, and productive catalytic capabilities.[47,48]

Spinel ferrite nanostructured $NiFe_2O_4$ has better magnetic properties, chemical inertness and reusability.[49] As a result, filtration or centrifugation processes are not required, since the material can be easily removed from the reaction mixtures using an external magnetic field. In addition, $NiFe_2O_4$ can also be used as an environmentally friendly catalyst, and the magnetic recoverability of the $NiFe_2O_4$ catalyst significantly reduces the loss of catalyst and makes it easy to recycle it.[50]

Additionally, the solvent-less ball milling process yields remarkably pure goods with no environmental impact.[51] The fact that the catalyst may be magnetically retrieved and reused without any activity loss demonstrates its economic and environmental benefits.[52]

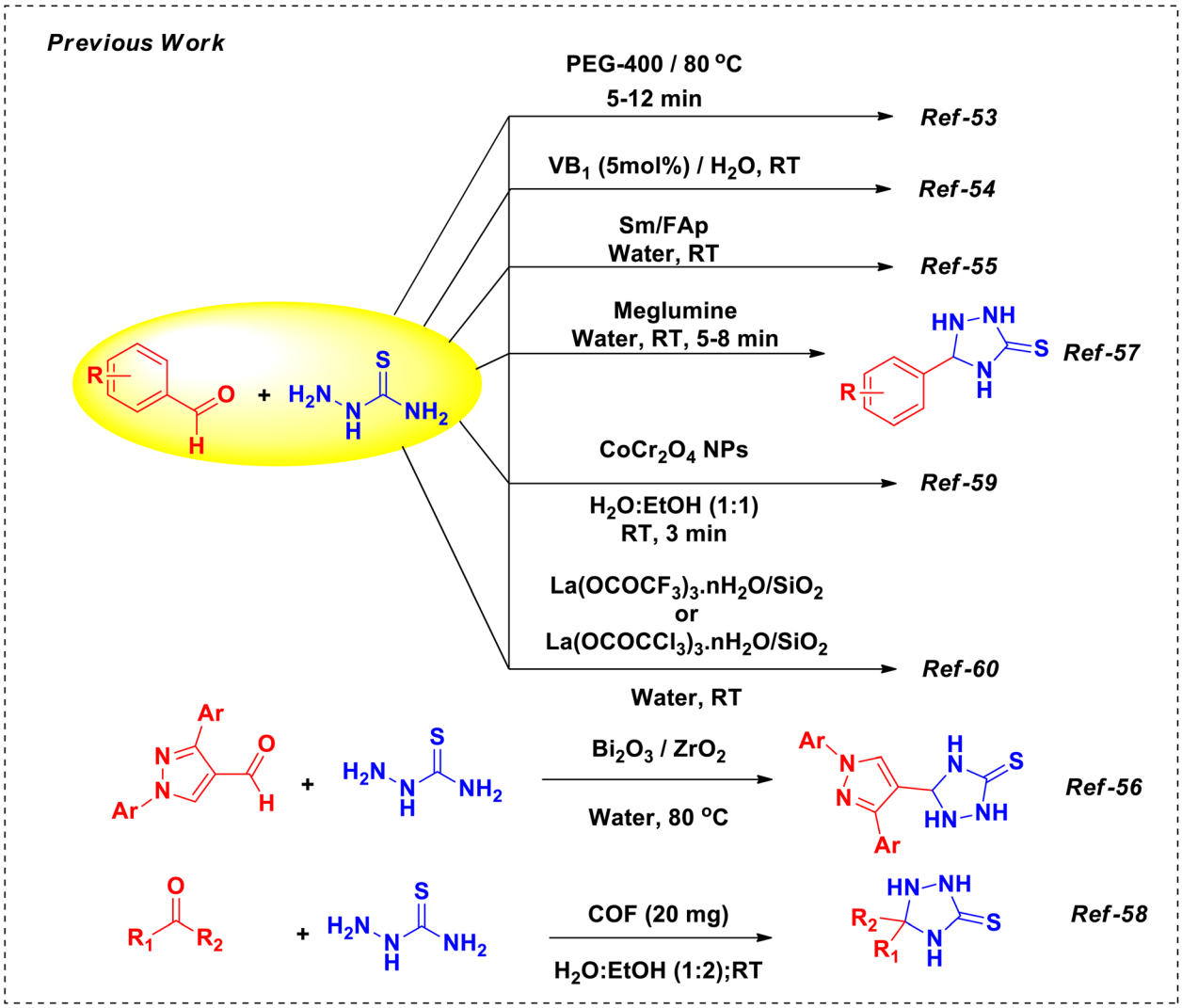

Scheme 1 Some previously reported substituted aryl-1,2,4-triazolidine-3-thiones.

In addition, the solvent-free ball-milling process produces extremely pure products that do not have any effect on the environment.[51] The economic and environmental benefits of the catalyst can be seen in the fact that the catalyst can be easily reused and recovered through a magnetic process without any significant activity loss.[52] Scheme 1 shows the previously reported synthesis of substituted aryl-1,2,4-triazolidine-3-thione scaffolds.[53–60]

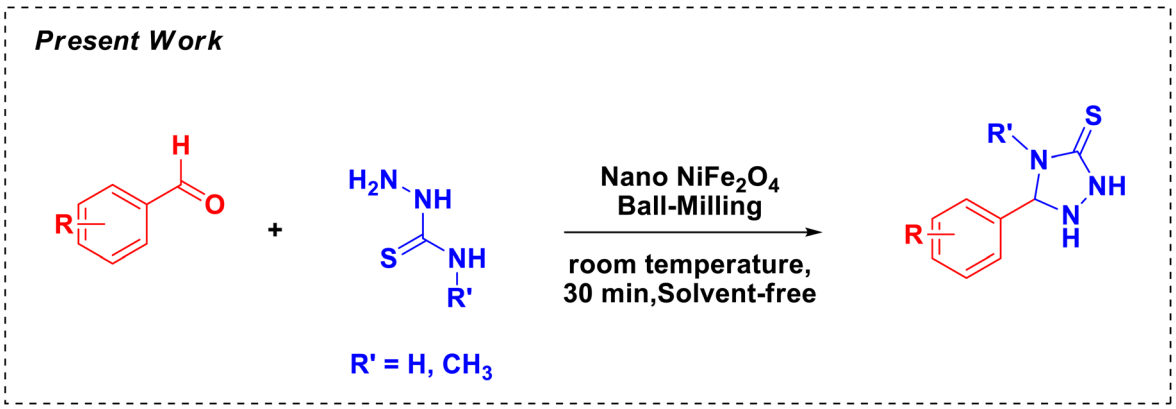

Scheme 2 Synthesis of 5-aryl-1,2,4-triazolidine-3-thiones.

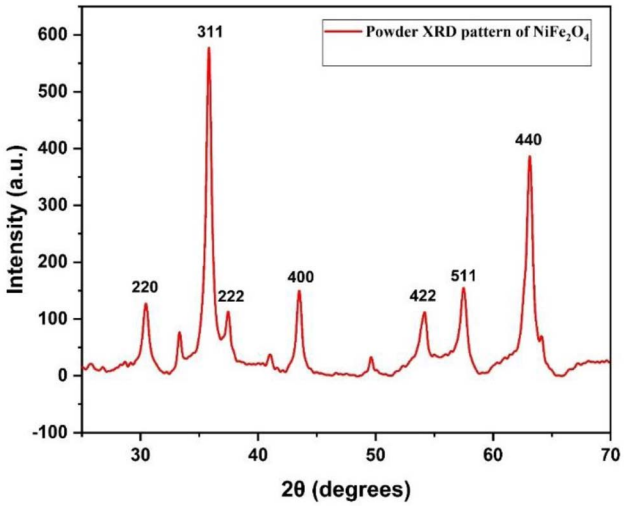

Fig. 2 The powder XRD pattern of nano-$NiFe_2O_4$.

This study aims to come up with a solvent-free mechanochemical reaction that makes use of nickel ferrite ($NiFe_2O_4$) nanoparticles as a recycling catalyst under ball-milling conditions for the formation of substituted-5-aryl-1,2,4-triazolidine-3-thiones, essential biological scaffolds that are progressively being synthesized using green chemistry (Scheme 2). This strategy would have offered a more efficient, green and fast alternative path to synthesis instead of dealing with the constraints of the traditional processes.

Synthetic compounds have considerable potential in pharmacological studies to be conducted in the future due to the anticipated high level of biological activity. This innovation opens up the frontiers of medicinal chemistry by merging mechanochemistry and magnetic nanocatalysts, making it possible to conduct sustainable heterocyclic synthesis.

The use of nanoscale $NiFe_2O_4$ as a heterogeneous catalyst using ball-milling conditions has been proven to be an innovative, environmentally benign methodology of synthesizing substituted-5-aryl-1,2,4-triazolidine-3-thione scaffolds. Typically, the activation of the functional groups found in the reactants and the facilitation of the intermolecular interactions are two synergistic processes that lead to bond formation through the collaboration of mechanical energy and nanocatalysis. These increases in yield and decrease in reaction time can be ascribed to the fact that the $NiFe_2O_4$ nanoparticles have surface Lewis acid sites that aid in both the process of condensation and cyclization.

2 Experimental section

2.1 Materials and methods

Chemicals needed were purchased from SRL, TCI, and ANCOTT and used without further purification. A Retsch agate grinding jar (250 mL) and planetary ball mill 100 (01.462.0220) have been used. Physical and chemical characterisation of all the identified products showed properties that were practically identical to those of the actual materials as demonstrated by ^{1}HNMR, ^{13}CNMR, FT-IR, and mass spectral characterisation. The melting points were determined with the help of a B-540. The data were collected using Bruker Avance Neo spectrometers at 500 MHz (SAIF, Chandigarh, India), and high-resolution mass spectrometry (HRMS) was also done. The FT-IR spectra were recorded using a SHIMADZU at R. T. M. Nagpur University, Nagpur.

2.2 Method for the preparation of $NiFe_2O_4$

The $NiFe_2O_4$ nanoparticles were synthesised *via* a straightforward sol–gel method[61] using readily available precursors: ferric chloride ($FeCl_3 \cdot 6H_2O$), nickel chloride ($NiCl_2 \cdot 6H_2O$), distilled water, and sodium hydroxide. In the typical procedure, a 0.2 M ferric chloride solution (20 mL) and a 0.1 M nickel chloride solution (20 mL) were prepared and mixed under vigorous stirring for 2 hours at 80 °C. Subsequently, 0.3 M NaOH was incrementally added until the pH reached 12, resulting in the formation of brown precipitates. The precipitates were then isolated through centrifugation and dried in a hot air oven for 4 hours at 100 °C, followed by calcination at 550 °C for 6 hours.

2.3 General procedure for synthesis of 5-aryl-1,2,4-triazolidine-3-thione scaffolds

2.3.1 Representative procedure for 5-phenyl-1,2,4-triazolidine-3-thione (3a, Table 5). Ball-milling was carried out using a 25 mL stainless steel beaker at a rotation rate of 600 rpm and took place for 30 minutes using six milling balls with a nominal diameter of 1/4 10 mm. In this process, nano-$NiFe_2O_4$

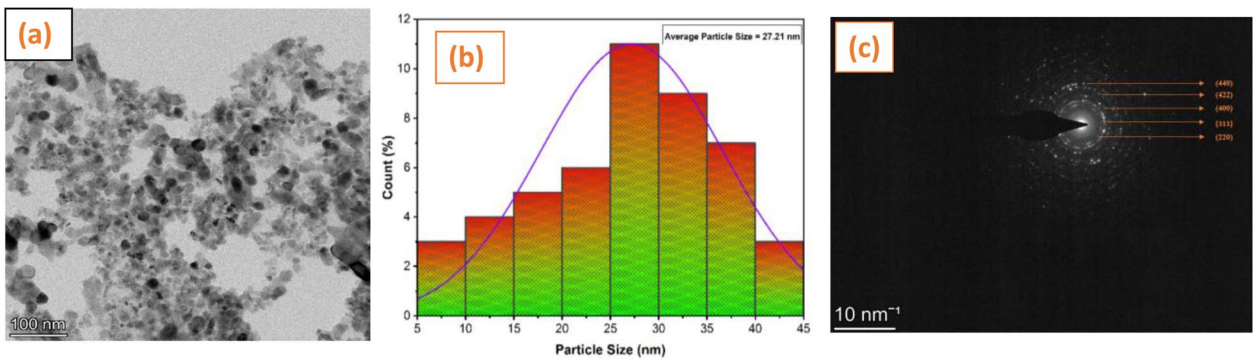

Fig. 3 HRTEM (a), histogram (b) and SAED pattern (c) of nano-$NiFe_2O_4$.

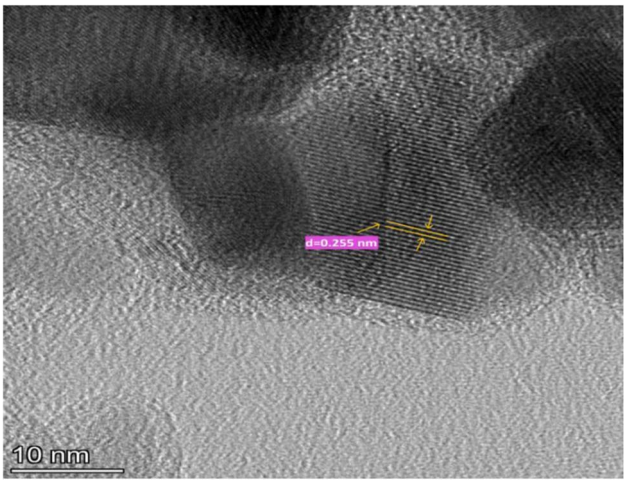

Fig. 4 Image of nano-$NiFe_2O_4$ displaying lattice fringes, magnified by HRTEM.

(10 mol%, 23.44 mg) as a catalyst was added to benzaldehyde **1a** (1.0 mmol, 106.12 mg) and thiosemicarbazide (1 mmol, 91.14 mg)/4-methylthiosemicarbazide (1 mmol, 105.17 mg). The operation of ball-milling was carried out by reversing directions of rotation, with a 30-second pause between consecutive sessions of milling. After the reaction was complete, an external magnet was used to collect the $NiFe_2O_4$ nanoparticles out of the reaction medium. The crude product (**3a**) was then recrystallized using ethanol. The recovered nano-$NiFe_2O_4$ was washed with a solution of ethanol and water, 1 : 1, after which it was dried in a hot-air oven at 60 °C for 1 hour. The catalyst was dried and reused in subsequent cycles of reaction.

3 Results and discussion

The powder XRD pattern (Fig. 2) indicates that the Bragg reflection peaks correspond to the face-centered cubic structure of $NiFe_2O_4$, classified under the *Fd3m* space group (JCPDS file No. 10-0325). The diffraction peaks at 30.35°, 35.76°, 37.38°, 43.44°, 53.93°, 57.44°, and 63.11° are associated with the {220}, {311}, {222}, {400}, {422}, {511}, and {440} planes of $NiFe_2O_4$, respectively. The average particle size, estimated using the Scherrer formula with XRD plane 311, is determined to be 21.98 nm. The high-resolution transmission electron microscopy (HRTEM) picture in Fig. 3(a) demonstrates the creation of spherical nano-$NiFe_2O_4$ with an average particle size of 27.21 nm, as shown in the histogram in Fig. 3(b). The selected area electron diffraction (SAED) pattern in Fig. 3(c) demonstrates the development of face-centered cubic spinel nano-$NiFe_2O_4$, with the corresponding planes {440}, {422}, {400}, {220}, and {311} accurately indexed, corroborating the findings from X-ray diffraction (XRD).

The magnified HRTEM picture (Fig. 4) of $NiFe_2O_4$ nanoparticles reveals lattice fringes with a spacing of 0.255 nm, corresponding to the (311) plane of $NiFe_2O_4$. The EDAX analysis (Fig. 5) reveals that the substance contains Fe, Ni, and O, with no other elements detected. The SEM picture of $NiFe_2O_4$ corroborated the presence of spherical particles (Fig. 6).

An inherent stretching vibration at 630 and 532 cm^{-1} was attributed to the tetrahedral site of ferrite (Fe–O), whereas 873 cm^{-1} was allocated to the Fe–OH group, as found in the FT-IR spectrum of nano-$NiFe_2O_4$ (Fig. 7).

The subsequent investigation focused on optimizing the reaction conditions for the synthesis of 5-phenyl-1,2,4-

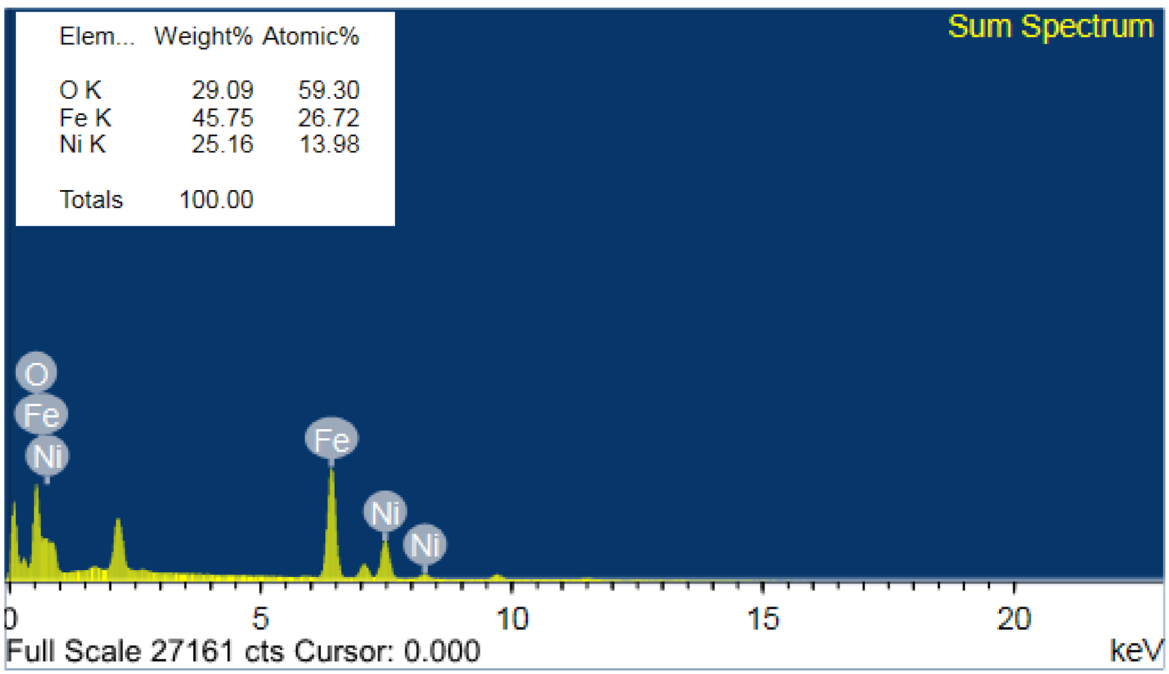

Fig. 5 EDS image of nano-$NiFe_2O_4$.

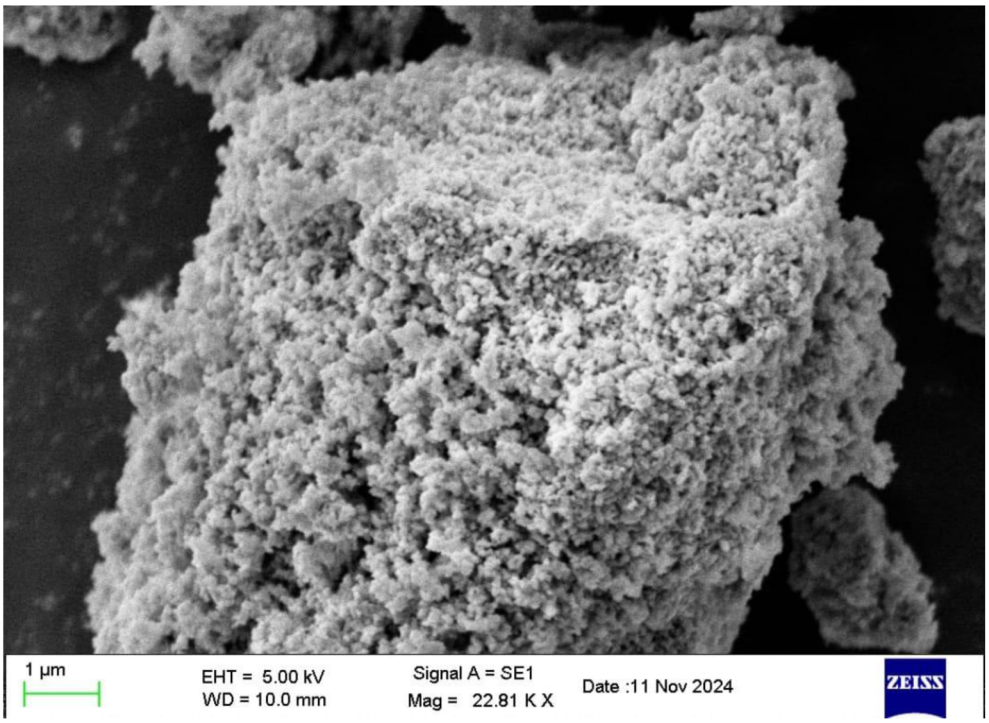

Fig. 6 SEM image of nano-$NiFe_2O_4$.

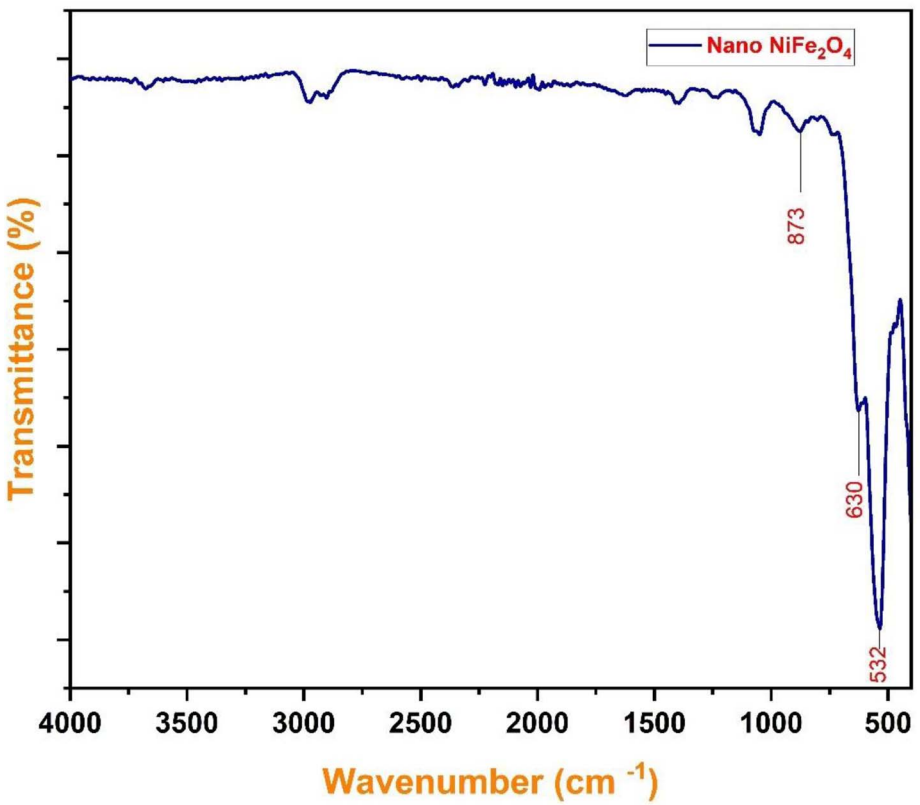

Fig. 7 FTIR spectrum of nano-$NiFe_2O_4$.

Table 1 Optimisation of reaction conditions[a]

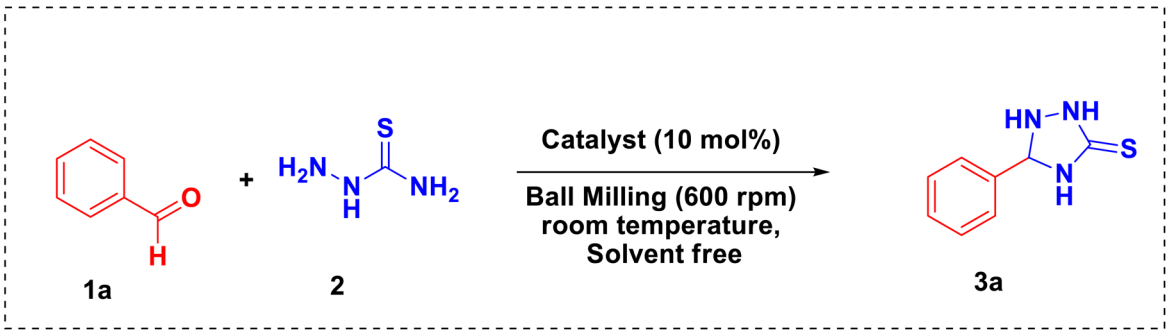

Entry	Products (**3a**)	Catalyst/additives	Time (min)	Catalyst (mol%)	Yield (%)[b]
1	Assembly (I)	$NiFe_2O_4$ NPs	15 min	5	35
2		$NiFe_2O_4$ NPs	20 min	5	41
3		$NiFe_2O_4$ NPs	25 min	5	44
4		$NiFe_2O_4$ NPs	30 min	5	57
5		$NiFe_2O_4$ NPs	35 min	5	59
6		$NiFe_2O_4$ NPs	40 min	5	63
7		$NiFe_2O_4$ NPs	45 min	5	66
8	**Assembly (II)**	$NiFe_2O_4$ NPs	15 min	10	78
9		$NiFe_2O_4$ NPs	20 min	10	81
10		$NiFe_2O_4$ NPs	25 min	10	88
11		**$NiFe_2O_4$NPs**	**30 min**	**10**	**97**
12		$NiFe_2O_4$ NPs	35 min	10	94
13		$NiFe_2O_4$ NPs	40 min	10	91
14		$NiFe_2O_4$ NPs	45 min	10	90
15	Assembly (III)	$NiFe_2O_4$ NPs	15 min	15	74
16		$NiFe_2O_4$ NPs	20 min	15	80
17		$NiFe_2O_4$ NPs	25 min	15	82
18		$NiFe_2O_4$ NPs	30 min	15	86
19		$NiFe_2O_4$ NPs	35 min	15	85
20		$NiFe_2O_4$ NPs	40 min	15	83
21		$NiFe_2O_4$ NPs	45 min	15	81
22	Assembly (IV)	$NiFe_2O_4$ NPs	50 min	10	88
23		$NiFe_2O_4$ NPs	55 min	10	85
24		$NiFe_2O_4$ NPs	60 min	10	83
25		$NiFe_2O_4$ NPs	60 min	15	87
26	Assembly (V)	$CoFe_2O_4$ NPs	30 min	10	22
27		$CuFe_2O_4$ NPs	30 min	10	25
28		Fe_3O_4 NPs	30 min	10	10
29		$ZnFe_2O_4$ NPs	30 min	10	22
30		No catalyst	30 min	—	NR

[a] Reaction conditions: benzaldehyde (1 mmol), thiosemicarbazide (1 mmol), solvent free, room temperature under ball-milling conditions (600 rpm), NR: not recovered. [b] Isolated yield.

triazolidine-3-thiones under ball milling conditions, as detailed in Table 1.

The product yield (**3a**) in assembly (I) was noted to be only 35% when the reaction between benzaldehyde and thiosemicarbazide was conducted using 5 mol% of $NiFe_2O_4$ NPs for a duration of 15 minutes under ball milling conditions at 600 rpm (entry 1, Table 1). As the reaction time is extended up to the range of 20 minutes to 45 minutes, the yield of product (**3a**) exhibits a gradual increase, from 41% to 66% (entry 2 to entry 7, Table 1), respectively.

It was found that the product yield (**3a**) in assembly (II) was only 78% when the reaction between benzaldehyde and thiosemicarbazide was conducted in the presence of 10 mol% of $NiFe_2O_4$ NPs in 15 minutes under ball milling conditions at 600 rpm (entry 8, Table 1). The longer the period of the reaction (20 minutes to 45 minutes), the higher the proportion of product (**3a**) in the reaction (entry 9 to entry 14, Table 1).

When 15 mol% of $NiFe_2O_4$ NPs was used to carry out the reaction between the benzaldehyde and thiosemicarbazide under 15 minutes of ball milling at 600 rpm (entry 15, Table 1), the product yield (**3a**) in assembly (III) was found to be only 74%. With an extended reaction period of a range of 20–45 minutes, there is a gradual increase in the yield of product 3a to 80 and 81 percent (entry 2 to entry 7, Table 1).

Upon extending the reaction time to 30 minutes and employing 10 mol% of $NiFe_2O_4$ nanoparticles as a catalyst,

Table 2 Effect of reaction conditions on the yield of **3a**

Entry	Catalyst	Catalyst (mole%)	Time (min)	Rotation (rpm)	Yield (%) [a]
1	$NiFe_2O_4$ NPs	5	30	400	51
2	$NiFe_2O_4$ NPs	5	30	500	54
3	$NiFe_2O_4$ NPs	5	30	600	57
4	$NiFe_2O_4$ NPs	10	30	400	95
5	$NiFe_2O_4$ NPs	10	30	500	96
6	**$NiFe_2O_4$NPs**	**10**	**30**	**600**	**97**
7	$NiFe_2O_4$ NPs	15	30	400	83
8	$NiFe_2O_4$ NPs	15	30	500	84
9	$NiFe_2O_4$ NPs	15	30	600	86
10	$NiFe_2O_4$ NPs	20	30	400	88
11	$NiFe_2O_4$ NPs	20	30	500	91
12	$NiFe_2O_4$ NPs	20	30	600	93

[a] Isolated yield, model reaction (3a): benzaldehyde (1.0 mmol), thiosemicarbazide (1.0 mmol) under ball milling conditions.

a maximum yield of 97% for product (**3a**) is achieved, as indicated in (entry 11, Table 1). Upon extending the reaction time to 50 min, 55 min, and 60 min in assembly (IV), a corresponding decrease in product yield was observed, with yields of 88%, 85%, and 83% respectively (entries 22, 23, and 24, Table 1).

The investigation of the same reaction utilizing various catalysts, specifically 10 mol% of $CoFe_2O_4$ NPs, $CuFe_2O_4$ NPs, Fe_3O_4 NPs, and $ZnFe_2O_4$ NPs, conducted for a duration of 30 minutes under ball milling conditions at 600 rpm *i.e.* optimised reaction conditions, reveals that no significant enhancement in the yield of product (**3a**) is noted (entry 26 to entry 29, Table 1). The reaction was not observed in the absence of a catalyst (entry 30, Table 1).

Analysis of the results presented in Table 1 indicates that $NiFe_2O_4$ nanoparticles exhibit superior catalytic activity for the formation of product (**3a**) when compared to $CoFe_2O_4$ nanoparticles, $CuFe_2O_4$ nanoparticles, Fe_3O_4 nanoparticles, and $ZnFe_2O_4$ nanoparticles. In this study, $NiFe_2O_4$ nanoparticles were chosen as a catalyst for the synthesis of 5-aryl-1,2,4-triazolidine-3-thiones under ball milling conditions.

Following the optimization of catalytic loading, the yield of the product (**3a**) was assessed at varying catalytic mol% and rpm under ball milling conditions (Table 2). The results indicate that the maximum yield of the product (**3a**) was achieved with 10 mole% of nano-$NiFe_2O_4$ at a rotational speed of 600 rpm (entry 6, Table 2).

In order to assess the effects of ball milling, a conventional reaction was performed. In a 25 mL round bottom flask, 1 mmol of benzaldehyde and 1 mmol of thiosemicarbazide were subjected to reflux in a solvent mixture of ethanol and water (1 : 1), utilizing 5–20 mole% of various $NiFe_2O_4$ nanoparticles as a catalyst (Table 3). Product (**3a**) was yielded by the reaction, but the yield was less than that of the ball milling conditions (see entry 11, Table 1). The reaction was not observed in the absence of a catalyst, and therefore, the product was not obtained in this control experiment (entry 30, Table 1).

Table 3 Comparison of nano-$NiFe_2O_4$-catalyzed conventional methodologies for the synthesis of **3a**

Entry	Catalyst	Catalyst (mol%)	Reaction conditions	Time (min)	Yield (%) [a]
1	$NiFe_2O_4$ NPs	5	Reflux/EtOH : H_2O (1 : 1)	30	22
2	$NiFe_2O_4$ NPs	5	Reflux/EtOH : H_2O (1 : 1)	60	30
3	$NiFe_2O_4$ NPs	5	Reflux/EtOH : H_2O (1 : 1)	90	38
4	$NiFe_2O_4$ NPs	5	Reflux/EtOH : H_2O (1 : 1)	120	43
5	$NiFe_2O_4$ NPs	10	Reflux/EtOH : H_2O (1 : 1)	30	50
6	$NiFe_2O_4$ NPs	10	Reflux/EtOH : H_2O (1 : 1)	60	55
7	$NiFe_2O_4$ NPs	10	Reflux/EtOH : H_2O (1 : 1)	90	57
8	$NiFe_2O_4$ NPs	10	Reflux/EtOH : H_2O (1 : 1)	120	56
9	$NiFe_2O_4$ NPs	15	Reflux/EtOH : H_2O (1 : 1)	30	52
10	$NiFe_2O_4$ NPs	15	Reflux/EtOH : H_2O (1 : 1)	60	54
11	$NiFe_2O_4$ NPs	15	Reflux/EtOH : H_2O (1 : 1)	90	56
12	$NiFe_2O_4$ NPs	15	Reflux/EtOH : H_2O (1 : 1)	120	55
13	$NiFe_2O_4$ NPs	20	Reflux/EtOH : H_2O (1 : 1)	30	50
14	$NiFe_2O_4$ NPs	20	Reflux/EtOH : H_2O (1 : 1)	60	51
15	$NiFe_2O_4$ NPs	20	Reflux/EtOH : H_2O (1 : 1)	90	49
16	$NiFe_2O_4$ NPs	20	Reflux/EtOH : H_2O (1 : 1)	120	52
17	No catalyst	—	Reflux/EtOH : H_2O (1 : 1)	90	NR

[a] Isolated yield, model reaction (**3a**): benzaldehyde (1.0 mmol), thiosemicarbazide (1.0 mmol) under conventional conditions, NR: not recovered.

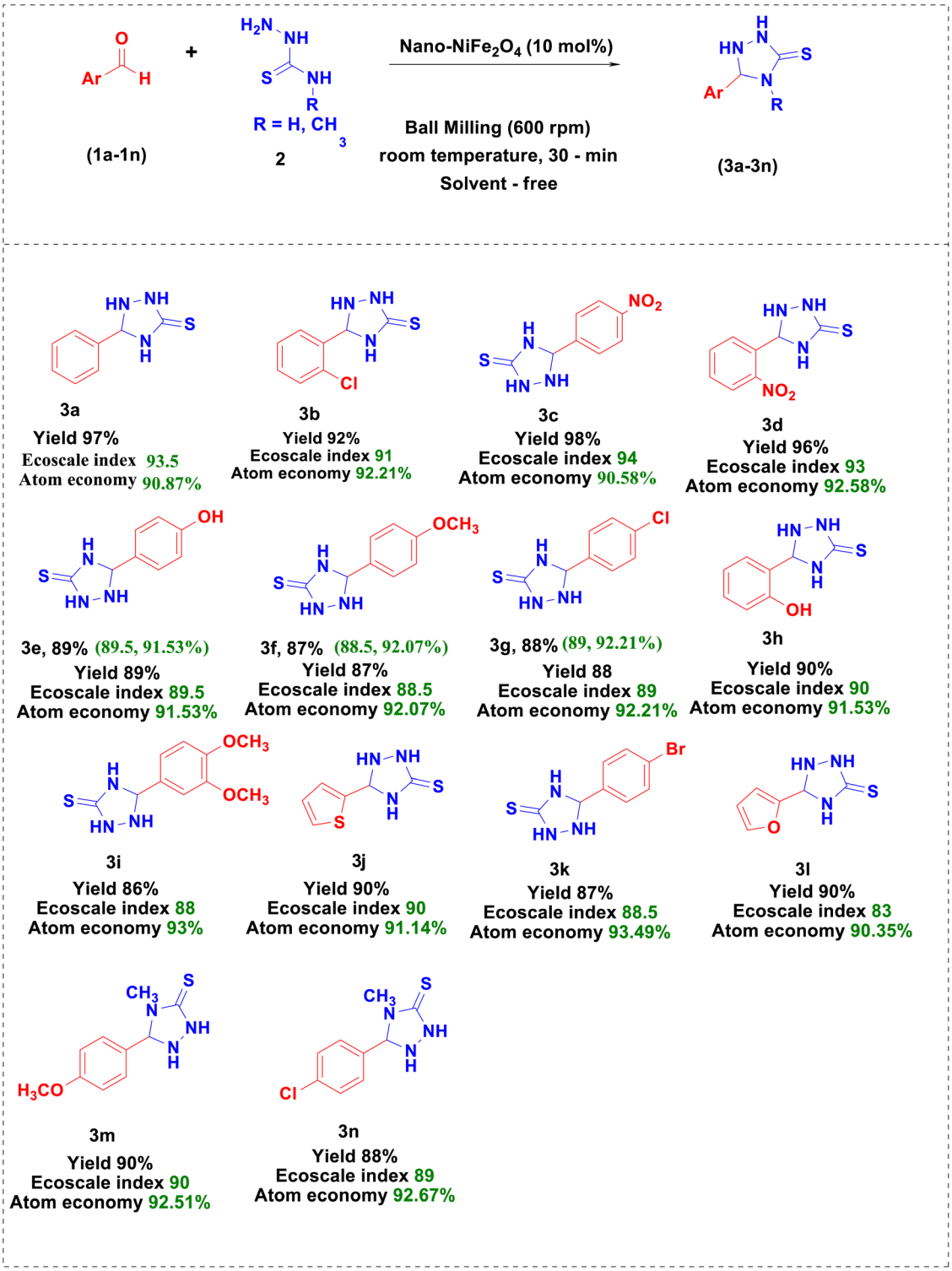

Scheme 3 Synthesis of substituted 5-aryl-1,2,4-triazolidine-3-thiones (**3a–3n**). Reaction conditions: a mixture of **1a** (1 mmol), 2 (1 mmol), and nano-$NiFe_2O_4$ (10 mol%). Yields refer to those of isolated products, EcoScale indices and atom economy respectively.

We have investigated the methods for the synthesis of a library of 5-aryl-1,2,4-triazolidine-3-thiones (**3a–3n**) utilizing optimum reaction conditions and a combination of thiosemicarbazide/4-methylthiosemicarbazide and different substituted aromatic aldehydes under ball milling conditions (Scheme 3). The reactions exhibited high levels of cleanliness, with yield percentages ranging from 86% to 98%. Upon completion of the reaction, the catalyst, in the form of nanoparticles (NPs), was isolated utilizing an external magnetic field. Subsequently, the NPs were subjected to washing with a mixture

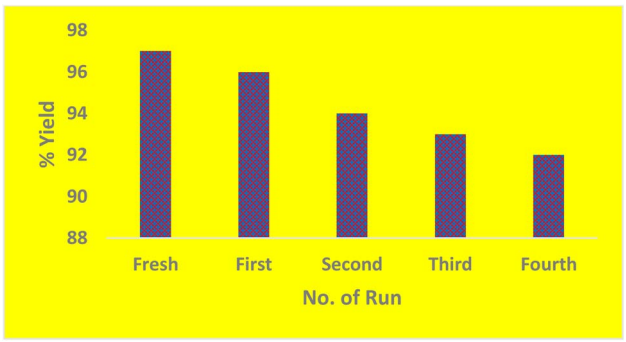

Fig. 8 Reusability study of the $NiFe_2O_4$ NP catalyst in the synthesis of **3a**.

of ethanol and water in a 1 : 1 ratio, followed by drying in a hot-air oven at 60 °C for a duration of 1 hour. The catalyst was then prepared for reuse in subsequent reactions. The synthesized products were further purified through washing with ethanol, resulting in analytically pure products. The synthesized products are subsequently validated through spectroscopic techniques, including FTIR, ^{1}H NMR, ^{13}C NMR, and HRMS (refer to the SI file).

Subsequently, an investigation was conducted to examine the reusability and stability of the $NiFe_2O_4$ nanoparticles in the synthesis of product (**3a**). Upon completion of the reaction, the catalyst was separated using a strong external magnet, followed by washing with a 1 : 1 mixture of ethanol and water. Subsequently, the catalyst was dried in a hot air oven at 60 °C for 1 hour. The catalyst that was recovered was subsequently employed in the model reaction, resulting in the production of (**3a**) with a yield of 97%. The catalyst was successfully recovered and subjected to recycling on three additional occasions, demonstrating a modest variation in product yield under the optimized reaction conditions, as illustrated in Fig. 8. An illustration of the HRTEM and histogram of the recycled catalyst can be found in Fig. 9. The average size of the particles has been established as 28.10 nm, which suggests that the structural stability is high up to the fourth cycle.

Motivated by these findings, we directed our efforts towards expanding the applicability of the protocol to include cyclic ketones and aryl ketones for the synthesis of the corresponding 1,2,4-triazolidine-3-thiones under the optimized reaction conditions. Regrettably, the acquisition of the product is not feasible at this time. This observation may be attributed to the reduced electrophilic character of the carbonyl carbon in ketones.

The catalytic transformation of benzaldehyde (**1a**) and thiosemicarbazide (**2**) into 5-phenyl-1,2,4-triazolidine-3-thione (**3a**) with the help of nano-$NiFe_2O_4$ is shown in Scheme 4. The benzaldehyde carbonyl moiety is activated at the onset by interaction with the Lewis-acidic sites (Ni^{2+}/Fe^{3+}) available at the surface of the nanocatalyst. This coordination enhances the electrophilicity of the carbonyl carbon, thus making it more susceptible to nucleophilic attack by the terminal –NH_2 group of the thiosemicarbazide. The resultant dehydration gives an imine intermediate. The milling process promotes the separation of the liberated water with the mechanical forces acting on it and shifts the equilibrium of the condensation process to product synthesis without the need to apply external heat or organic solvents. These are then followed by intramolecular nucleophilic attack of the thiosemicarbazide nitrogen on the imine carbon, leading to ring closure. The resultant system is further subjected to tautomerization and rearrangement eventually affording the substituted-5-aryl-1, 2,4-triazolidine-3-thione.

In adherence to the principles of green chemistry, we assess various green parameters, including the EcoScale, E-factor, and atom economy, which serve to evaluate the greenness, efficiency, and sustainability of the reaction (refer to the SI file).

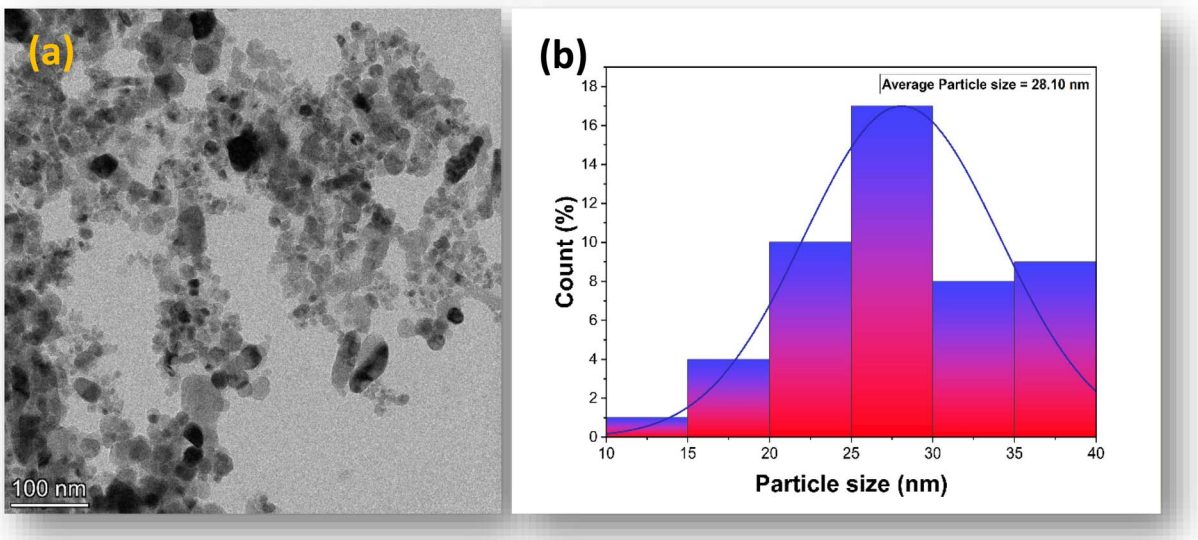

Fig. 9 HRTEM (a) and the histogram (b) of reused nano-$NiFe_2O_4$.

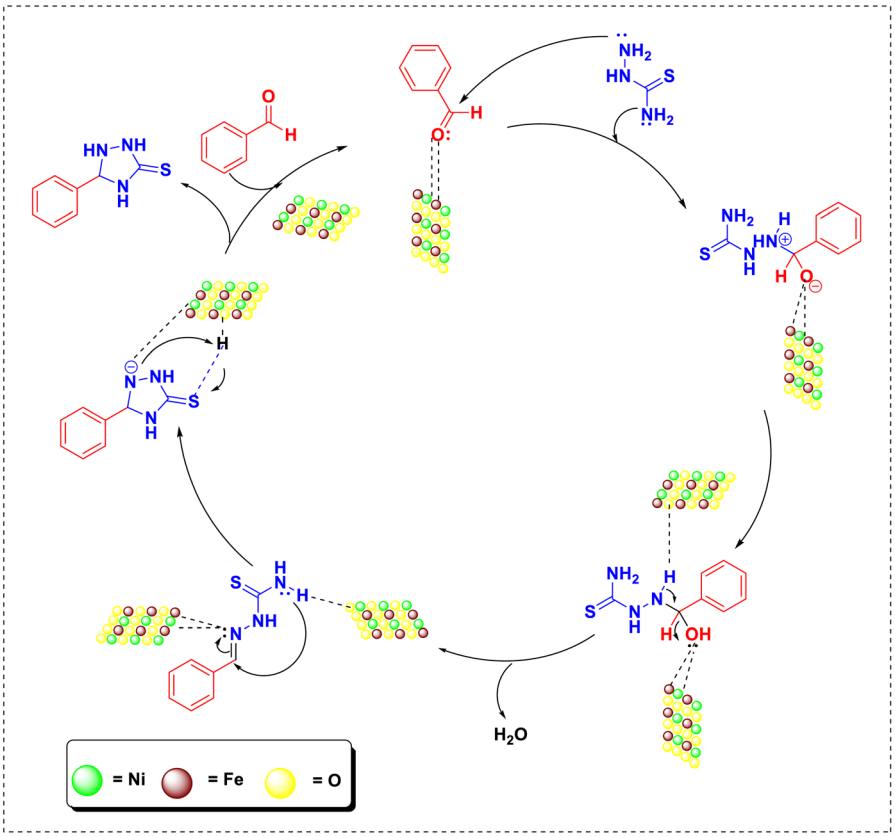

Scheme 4 Plausible mechanistic pathway for synthesis of 5-phenyl-1,2,4-triazolidine3-thione.

Green measuring tools like Eco-Scale and E-factor show that the mechanochemical protocol complies with the principles of green chemistry. The Eco-Scale, which is commonly used to determine the generality and operational simplicity of an approach, provides quantitative scores that describe the overall effectiveness of the process. The E-factor is a dimensionless measure that combines waste production with ancillary factors such as cost, safety, technological infrastructure, energy use and purification needs to give a holistic picture of the environmental impact. Table 4 shows the calculated values of the Eco-Scale of the synthesis of compounds (**3a–3n**). All the entries exceed a mark of 80, which supports a high sustainability rating of the procedure (see the SI; Table 4). These green metrics are calculated in detail in the SI; the E-factor of synthesizing compound (**3a**) is 0.13. Compared with a traditional thermal approach, the mechanochemical approach produced a better Eco-Scale value and a lower E-factor.

4 Conclusion

Finally, the direct and cost-effective preparation of 5-aryl-1,2,4-triazolidine-3-thione was made possible by the use of nano-$NiFe_2O_4$ in ball-milling reactions as a recyclable catalyst. The activation of the carbonyl functionality of the acidic Lewis site of nano-$NiFe_2O_4$ initiated a sequence of reactions, which was followed by condensation and then by the nucleophilic attack to accomplish ring closure. The current methodology enables high rates of transformations (30 min), high isolated yields (86–98%) and catalyst reusability; ball-milling allows high yielding protocols to be performed expeditiously.

Conflicts of interest

There are no conflicts to declare.

Data availability

All data that support the findings of this study are included in the article.

Supplementary information (SI) is available. See DOI: https://doi.org/10.1039/d6na00160b.

Acknowledgements

The author, P. V. Ledade, gratefully appreciates the Principal, SSES Amravati's Science College, Congress Nagar, Nagpur, for providing excellent research facilities and SAIF Chandigarh for NMR and HRMS analysis.

References

1 A. Al-Mulla, *Der Pharma Chemica*, 2017, **9**, 141–147.
2 E. Kabir and M. Uzzaman, *Results Chem.*, 2022, **4**, 100606.

3 P. K. Shukla, A. Verma and P. Mishra, *New Perspective in Agricultural and Human Health*, 2017, p. 100.
4 N. N. Makhova, L. I. Belen'kii, G. A. Gazieva, I. L. Dalinger, L. S. Konstantinova, V. V. Kuznetsov, *et al.*, *Russ. Chem. Rev.*, 2020, **89**, 55.
5 P. K. Sharma, A. Amin and M. Kumar, *Open Med. Chem. J.*, 2020, **14**, 49–64.
6 (*a*) M. Ajmal, A. K. Mahato, M. Khan, S. Rawat, A. Husain, E. B. Almalki, *et al.*, *Chem. Biodiversity*, 2024, **21**, e202400637; (*b*) P. K. Hazarika, P. Gogoi, S. Sarmah, B. Das, K. Deori, D. Sarma, *et al.*, *RSC Sustain.*, 2024, **2**, 1782–1796; (*c*) P. Gogoi, M. Rahman, R. Hazarika, B. Das, K. Deori, D. Sarma, *et al.*, *New J. Chem.*, 2024, **48**, 16609–16619; (*d*) P. K. Hazarika, P. Gogoi, R. Hazarika, K. Deori, D. Sarma, *et al.*, *Mater. Adv.*, 2022, **3**, 7810–7814.
7 Q. Guan, S. Xing, L. Wang, J. Zhu, C. Guo, C. Xu, *et al.*, *J. Med. Chem.*, 2024, **67**, 7788–7824.
8 V. Gupta, R. Ambatwar, N. Bhanwala and G. L. Khatik, *Curr. Top. Med. Chem.*, 2023, **23**, 1489–1502.
9 R. Nishanth Rao, S. Jena, M. Mukherjee, B. Maiti and K. Chanda, *Environ. Chem. Lett.*, 2021, **19**, 3315–3358.
10 S. S. Gupta, S. Kumari, I. Kumar and U. Sharma, *Chem. Heterocycl. Compd.*, 2020, **56**, 433–444.
11 (*a*) A. Shanmugapriya, F. Dallemer and R. Prabhakaran, *New J. Chem.*, 2018, **42**, 18850–18864; (*b*) S. Teli, S. Soni, N. Rana, A. Manhas, S. Agarwal, *et al.*, *Nanoscale Adv.*, 2025, **7**, 8104–8121.
12 K. K. Gangu, S. Maddila, S. N. Maddila and S. B. Jonnalagadda, *Molecules*, 2016, **21**, 1281.
13 M. A. Elzoheiry, M. S. Elmehankar, W. A. Aboukamar, R. El-Gamal, H. Sheta, D. Zenezan, N. Nabih and A. A. Elhenawy, *Exp. Parasitol.*, 2022, **239**, 108291.
14 B. Burman, S. B. Drutman, M. G. Fury, R. J. Wong, N. Katabi, A. L. Ho and D. G. Pfister, *Oral Oncol.*, 2022, **128**, 105806.
15 H. G. Park, J. H. Kim, A. N. Dancer, K. S. Kothapalli and J. T. Brenna, *Prostaglandins, Leukotrienes Essent. Fatty Acids*, 2021, **171**, 102312.
16 A. A. Ziyaev, S. A. Sasmakov, T. T. Toshmurodov, J. M. Abdurakhmanov, S. A. Ikramov, S. S. Khasanov, *et al.*, *Organics*, 2025, **6**, 41.
17 B. A. Baviskar, S. S. Khadabadi and S. L. Deore, *J. Chem.*, 2013, **2013**, 656271.
18 (*a*) M. Mustafa and J. Y. Winum, *Expert Opin. Drug Discov.*, 2022, **17**, 501–512; (*b*) S. Gudala, A. Sharma, A. Lankada, R. Liu, A. Jha, S. Penta, *et al.*, *ACS Omega*, 2024, **9**, 38262–38271.
19 R. R. Mane and K. Kamanna, *Curr. Organocatalysis*, 2025, **12**, 177–190.
20 C. Hansch, A. Leo and R. W. Taft, *Chem. Rev.*, 1991, **91**, 165–195.
21 M. W. Holladay, *Drug Dev. Res.*, 2015, **75**, 471–472.
22 A. A. Aly, A. A. Hassan, M. M. Makhlouf and S. Bräse, *Molecules*, 2020, **25**, 3036.
23 F. Shaikh, S. L. Shastri, N. S. Naik, R. Kulkarni, J. M. Madar, L. A. Shastri, *et al.*, *ChemistrySelect*, 2019, **4**, 105–115.
24 A. Sharma, R. Bhutani, A. Gupta and M. Dutta, *Comb. Chem. High Throughput Screening*, 2026, **29**, 20–32.
25 R. N. Okigbo, C. L. Anuagasi, J. E. Amadi and U. J. Ukpabi, *Int. J. Integr. Biol.*, 2009, **6**, 91–98.
26 P. G. Mahajan, N. C. Dige, B. D. Vanjare, H. Raza, M. Hassan, S. Y. Seo, *et al.*, *Mol. Diversity*, 2020, **24**, 1185–1203.
27 A. A. Ziyaev, S. A. Sasmakov, T. T. Toshmurodov, J. M. Abdurakhmanov, S. A. Ikramov, S. S. Khasanov, *et al.*, *Organics*, 2025, **6**, 41.
28 H. A. Almasmoum, G. Almaimani, R. A. Almaimani, A. T. Babakr, M. Alsunbul, H. A. Alshwyeh, *et al.*, *RSC Adv.*, 2025, **15**, 24769–24790.
29 S. Shohag, S. Akhter, S. Islam, T. Sarker, M. K. Sifat, M. M. Rahman, *et al.*, *Oxid. Med. Cell. Longev.*, 2022, **2022**, 7743705.
30 T. Glomb, J. Minta, M. Nowosadko, J. Radzikowska and P. Świątek, *Molecules*, 2024, **29**, 6036.
31 S. Mujeeb, K. Singh, B. Yogi, V. Ansari and S. Sinha, *Mini-Rev. Med. Chem.*, 2022, **22**, 1064–1080.
32 I. Serrano, C. Verdial, L. Tavares and M. Oliveira, *Antibiotics*, 2023, **12**, 505.
33 W. M. Huggins, B. M. Minrovic, B. W. Corey, A. C. Jacobs, R. J. Melander, R. D. Sommer, *et al.*, *ACS Med. Chem. Lett.*, 2017, **8**, 27–31.
34 M. Gopalakrishnan, V. Kanagarajan and J. Thanusu, *Green Chem. Lett. Rev.*, 2008, **1**, 241–246.
35 M. Patil, P. Mhaldar, V. Mahadik and D. M. Pore, *Tetrahedron Lett.*, 2020, **61**, 152015.
36 (*a*) S. Kar, H. Sanderson, K. Roy, E. Benfenati and J. Leszczynski, *Chem. Rev.*, 2021, **122**, 3637–3710; (*b*) G. Patel, A. R. Patel, T. L. Lambat, S. H. Mahmood and S. Banerjee, *FlatChem*, 2020, **21**, 100163; (*c*) G. Patel, A. R. Patel, T. L. Lambat and S. Banerjee, *Curr. Res. Green Sustain. Chem.*, 2021, **4**, 100149.
37 (*a*) A. Cannon, S. Edwards, M. Jacobs, J. W. Moir, M. A. Roy and J. A. Tickner, *RSC Sustain.*, 2023, **1**, 2092–2106; (*b*) P. Gogoi, H. Deka, B. Das, K. Deori, D. Sarma, *et al.*, *ACS Sustain. Chem. Eng.*, 2024, **13**, 936–945; (*c*) P. V. Ledade and T. L. Lambat, *Curr. Org. Chem.*, 2023, **27**(3), 223–241.
38 G. W. Wang, *Chem. Soc. Rev.*, 2013, **42**, 7668–7700.
39 F. Basoccu, L. De Luca and A. Porcheddu, *Eur. J. Org Chem.*, 2024, **27**, e202400425.
40 K. Roy, S. Sahoo, A. Saha and L. Adak, *Curr. Org. Chem.*, 2023, **27**, 153–165.
41 (*a*) C. Xu, S. De, A. M. Balu, M. Ojeda and R. Luque, *Chem. Commun.*, 2015, **51**, 6698–6713; (*b*) P. S. Gaikar, *et al.*, *Nanoscale Adv.*, 2022, **4**(24), 5245–5252.
42 I. N. Egorov, S. Santra, D. S. Kopchuk, I. S. Kovalev, G. V. Zyryanov, A. Majee, *et al.*, *Green Chem.*, 2020, **22**, 302–315.
43 S. L. James, C. J. Adams, C. Bolm, D. Braga, P. Collier, T. Friščić, *et al.*, *Chem. Soc. Rev.*, 2012, **41**, 413–447.
44 N. Mukherjee, P. Maity and B. C. Ranu, in *Green Synthetic Approaches for Biologically Relevant Heterocycles*, Elsevier, 2021, pp. 167–187.
45 C. Xu, S. De, A. M. Balu, M. Ojeda and R. Luque, *Chem. Commun.*, 2015, **51**, 6698–6713.
46 Y. Jiang, J. Liang, F. Zhuo, H. Ma, S. S. Mofarah, C. C. Sorrell, *et al.*, *ACS Nano*, 2025, **19**, 18037–18074.

47 H. Zhao, Y. Dong, G. Wang, P. Jiang, J. Zhang, L. Wu and K. Li, *Chem. Eng. J.*, 2013, **219**, 295–302.
48 V. Singh, *Int. J. New Chem.*, 2025, **12**, 283–317.
49 E. E. Ateia, S. Fouad and A. T. Mohamed, *Appl. Phys. A*, 2025, **131**, 980.
50 (*a*) P. N. Anantharamaiah, S. Mondal, K. S. Manasa, S. Saha and M. Pai, *Ceram. Int.*, 2020, **46**, 1220–1226; (*b*) T. L. Lambat, *Results Chem.*, 2023, **6**, 101176.
51 P. Pattanayak, S. Saha, T. Chatterjee and B. C. Ranu, *Chem. Commun.*, 2025, **61**, 247–265.
52 V. Polshettiwar, R. Luque, A. Fihri, H. Zhu, M. Bouhrara and J. M. Basset, *Chem. Rev.*, 2011, **111**, 3036–3075.
53 R. Ramesh and A. Lalitha, *RSC Adv.*, 2015, **5**, 51188–51192.
54 P. J. Patil, G. D. Salunke, M. B. Deshmukh, S. P. Hangirgekar, D. R. Chandam and S. A. Sankpal, *ChemistrySelect*, 2019, **4**, 13071–13078.
55 S. N. Maddila, S. Maddila, K. K. Gangu, W. E. van Zyl and S. B. Jonnalagadda, *J. Fluorine Chem.*, 2017, **195**, 79–84.
56 N. Kerru, S. V. Bhaskaruni, L. Gummidi, S. N. Maddila, P. Singh and S. B. Jonnalagadda, *Mol. Diversity*, 2020, **24**, 345–354.
57 L. B. Masram, S. S. Salim, A. B. Barkule, Y. U. Gadkari and V. N. Telvekar, *J. Chem. Sci.*, 2022, **134**, 94.
58 P. Teli, S. Soni, S. Teli and S. Agarwal, *Nanoscale Adv.*, 2024, **6**, 5568–5578.
59 S. Ghotekar, D. Sanap, K. Y. A. Lin, H. Louis, D. Pore and R. Oza, *Res. Chem. Intermed.*, 2024, **50**, 49–68.
60 D. P. Gholap, R. Suradkar, R. Huse, A. Belambe and M. K. Lande, *ACS Omega*, 2025, **10**, 37176–37187.
61 S. Shylesh, V. Schünemann and W. R. Thiel, *Angew. Chem., Int. Ed.*, 2010, **49**, 3428–3459.